Microscopy in addition to chemical analyses and ecotoxicological assays for the environmental hazard assessment of coal tar-polluted soils

Christine Lors, Jean-François Ponge, Denis Damidot

Microscopy in addition to chemical analyses and ecotoxicological assays for the environmental hazard assessment of coal tar polluted soils

Christine Lors[1*], Jean-François Ponge[2], Denis Damidot[1]

[1]IMT Lille Douai, Univ. Lille, EA 4515 – LGCgE – Laboratoire de Génie Civil et Géoenvironnement, Département Génie Civil & Environnemental, 941 rue Charles-Bourseul, 59508 Douai, France

[2]Muséum National d'Histoire Naturelle, CNRS UMR 7179, 4 Avenue du Petit Château, 91800 Brunoy, France

Abstract Chemical analysis of soils contaminated with coal tar indicated that most organic compounds, and particularly PAHs, were contained in coarser particles (> 200 µm). Microscopic observations of this fraction, carried out on polished sections, reported the presence of organic particles in addition to mineral particles. Some organic particles had a very low porosity and their microstructure did not evolve during biotreatment. Alternatively, other organic particles had a large porosity composed of an interconnected pore network that was open to coal tar surface and thus in contact with soil water. Interconnected porosity seemed to increase during biotreatment in relation to a decrease in the amount of organic compounds. The amount of open porosity in contact with soil water was expected to increase the desorption rate of PAHs. Consequently, the environmental hazard could depend on the amount of open porosity in addition to chemical properties of organic particles, such as their concentration in PAHs. Thus, microscopy can be complementary to chemical analysis and ecotoxicological assays to assess the best strategy for remediation but also to follow the advancement of a biotreatment.

Keywords Coal tar; PAHs; Environmental hazard assessment; Ecotoxicity; Pore network; Microscopy

[*] Corresponding author: E-mail: christine.lors@imt-lille-douai.fr, Phone +33 3 27712674

Introduction

Industrial activities have led to the discharge of a wide range of hazardous chemical in soils, such as coal tar that contains Non-Aqueous Phase Liquids (NAPLs). The composition of coal tar varies widely depending on its origin (Brown et al. 2006). Nevertheless, coal tars are always composed of hundreds of organic compounds but also of some inorganic constituents. Main organic compounds are polynuclear aromatic hydrocarbons (PAHs), phenolic compounds, such as cresols, BTEX as well as aliphatic and polar hydrocarbons (EPRI 1993). The microstructure of coal tars and their cokes is complex and also varies markedly according to processing conditions. Some more or less anisotropic textures are found along with variable amounts of porosity (Panaitescu and Predeanu 2007; Picon-Hernandez et al. 2008).

Most organic substances contained in coal tars are potentially toxic, mutagenic and carcinogenic (White and Claxton 2004). Thus, once soils have been polluted by coal tar, it is important to assess their environmental risk and try to suppress or at least to mitigate it. Some remediation techniques are applied, such as bioremediation that is often used to cure PAH-contaminated soils (Johnsen et al. 2005). Finally, the efficiency of a treatment also requires the evaluation of post-treatment environmental risk.

Microbial degradation, one of the most important processes of PAH destruction in soils, has been extensively studied. The transfer of PAHs from coal tar to soil water is the first critical step before PAHs can be metabolized (Mahjoub et al. 2000; Nambi and Powers 2000; Semple et al. 2003; Benhabib et al. 2010). Thus, PAH availability to microorganisms depends primarily on PAH transfer rate that is controlled by several mechanisms, such as (*i*) the diffusion of PAHs from coal tar to soil water, (*ii*) the solubility of PAHs that decreases with increasing number of rings, (*iii*) the contact surface of coal tar in soil water, and (*iv*) soil properties. The surface of coal tar particles in contact with soil water depends on their shape, size and distribution in the different soil fractions (Chung and Alexander 2002; Vulava et al. 2007; Al-Raoush 2014). However, despite of the importance of coal tar microstructure in the bioremediation process, microscopic observations of coal tar in polluted soils are scarce (Ghosh et al. 2000). A precise description of polluted soils is also infrequent despite its usefulness to better understand the physicochemical processes involved. For example, PAH availability to microorganisms can be reduced if PAHs are adsorbed to some compounds of the soil, such as organic matter or clay particles, which protect them from degradation (Vulava et al. 2012). Consequently, higher microbial degradation rates occur in soils with lower amounts of soil organic matter and clay (Thiele-Bruhn and Brümmer 2004; Rhodes et al. 2008).

Considering the complexity of the mechanisms involved, environmental risk is thus often

assessed by a global approach thanks to ecotoxicological bioassays. These bioassays indirectly assess the bioavailability of PAHs in polluted soils (Peijnenburg et al. 2002; Eom et al. 2007; Riding et al. 2013). However, bioassays are not compound-specific and the availability of pollutants is also specifically linked to soil properties (Riding et al. 2013). PAH bioavailability is thus related to the fraction actually available for the organisms used in the bioassay.

The present work aimed at further assessing the environmental hazard of three soils polluted by coal tar that was previously estimated by an ecoscore calculated from a complete battery of acute and chronic toxicity bioassays (Lors et al. 2010, 2011). In these previous studies, ecotoxicity assessed by ecoscores was not connected with the total concentration of PAHs. A more precise study of these three soils was thus performed to bring further explanations for the reported differences. First, a chemical analysis was performed on several fractions of each soil to assess how coal tar particles and PAHs were distributed. Second, a special attention was paid to the observation of the microstructure of coal tar particles by several microscopic techniques. Finally, the impact of both PAHs concentration in coal tar particles and their microstructure was discussed with respect to the desorption rate of PAHs, and consequently to environmental hazard assessment.

Material and methods

Soil samples

Experiments were carried out on three coal tar-contaminated sandy soils sampled from two historical industrial sites located in the North of France, in which the distillation of coal tar was the main activity. Properties of these soils were detailed in previous papers (Lors et al. 2010, 2011). Briefly, a soil was collected in one of the two sites, before (soil S3) after 6-month windrow biotreatment (soil S3T), while soil S2 was collected in another site after 18-month windrow biotreatment.

Chemical and ecotoxicological analyses

The three sandy soils were separated into six fractions: < 2, 2-20, 20-50, 50-200, 200-2000, and > 2000 µm. The first three fractions were obtained by dry sieving using sieves between 50 and 200 µm. The smaller fractions (< 50 µm) were obtained by moist way, at first by sieving soil under water through a sieve of 20 µm. The fraction retrieved on the sieve, corresponding to the fraction 20-50 µm, was dried to 30°C. The filtrate suspension, corresponding to the fraction < 20 µm, was

centrifuged to 1000 rpm during 3.5 min, enabling us to separate fractions 2-20 µm and < 2 µm. The different fractions were dried at 30°C, then analysed to measure the concentration of the 16 PAHs of the US-EPA list according to ISO 13877 (ISO 1998) and the total organic carbon (TOC) concentration according to ISO 10694 (ISO 1995). Additionally, the mineral composition of the soils was studied by X-ray diffraction.

Ecotoxicity was evaluated with the help of ecoscores, based on a restricted array of biological endpoints. The calculation of ecoscores has been detailed in Lors et al. (2010, 2011, 2017). The set of bioassays was selected by Lors et al. (2011) from nine bioassays tested on the basis of their best sensitivity to PAH pollution. This set of bioassays included both solid and liquid phases and addressed acute and chronic toxicities and genotoxicity: two rapid bioassays (Microtox® and springtail avoidance), a micronucleus test and three bioassays of a longer duration (algal growth, lettuce germination and springtail reproduction).

Microscopic observations of soil samples

The soil fraction larger than 200 µm was prepared, in order to be observed by scanning electron microscopy and by optical microscopy. The soil fraction was impregnated under vacuum with epoxy resin in circular moulds (diameter: 2 cm). After hardening of the epoxy resin, the surface was pre-polished under water using several diamond-covered polishing discs having a decreasing particle size: 151, 75, 46 and 16 µm. To obtain a flat surface prior to fine polishing steps, samples were polished using a silicon carbide grinding wheel (particle size: 8 µm). The fine polishing steps were performed using diamond pastes of decreasing particle size (9, 6, 3, 1, ½, and ¼ µm). Samples were gold coated before observation under a scanning electron microscope (Hitachi S-4300SE/N) operating in backscattered electron (BSE) mode (20 KeV and 2 KA). Elemental chemical analysis was performed with a Thermoscientific Ultradry EDX detector running at 15 kV. Complementary experiments carried out with an optical microscope (Leica DMRXP) under reflected light were performed directly on uncoated samples. Image analysis of BSE images was performed using a specific procedure adapted from the statistical analysis of BSE images performed on hydrated cement paste (Hu and Ma. 2016). First, one hundred coal tar particles were cut manually using Adobe Photoshop® from several BSE images (3968 x 2232 pixels) taken at a magnification of 100 x. Then, each digital coal tar particle was pasted in a separate rectangular image having a white background colour. The total surface of coal tar particles was estimated by counting the number of pixels having a level of grey different than white, using a MATLAB® procedure. Then, coal tar images were segmented based on grey levels of pixels associated to the organic compounds of coal tar. Indeed, the contrast organic phases, pore-intruding resin, empty

pores and mineral phases contained in the pores of coal tar particles was sufficient to easily depict organic compounds. The content of organic compounds was determined by dividing the pixels of segmented images by the total pixels of coal tar particles. Finally, the porosity of coal tar grains was equal to the surface fraction that was not attributed to organic compounds. As 100 coal tar particles were treated by image analysis for each soil, the surface fractions of coal tar particle components were equal to their volume fraction (Igarashi et al., 2004).

Results

Chemical analysis of soils as a function of soil fractions

The biotreatment decreased PAH and total organic carbon (TOC), resulting in decreased ecotoxicity, as expected (Fig. 1). However, soil S2 was much less ecotoxic than soil S3 despite its higher amount of PAHs (Lors et al. 2017).

For all three soils, the fraction larger than 200 µm (> 200 µm) represents more than 70% of the soil mass (Table 1). From a mineralogical point of view, all soils are mostly composed of quartz with some feldspar as minor phase and traces of clay in accordance with the sandy nature of the soils. The windrow treatment (S3T versus S3) did not alter the distribution of the different mineral fractions. In all three soils the fraction 200-2000 µm contains the majority of total soil organic carbon (TOC) and PAHs (Tables 2-4).

The advancement of the microbial degradation of PAHs contained in coal tar particles can be estimated by considering the relative amount of most soluble (better bioavailable, with a lower number of rings) over less soluble PAHs (Bamforth and Singleton 2005). This parameter, noted as 2-4/5-6 ratio, was calculated by dividing the concentrations of 2-4-ring PAHs by the concentrations of 5-6-ring PAHs. This ratio is thus expected to decrease with the advancement of degradation. The concentration of 5-6-ring PAHs is high relatively to 2-4-ring PAHs in all fractions of soil S2 (2-4/5-6 ratio ranging from 0.83 to 1.55), in agreement with its previous windrow treatment (Table 2), although a comparison with this soil previous to 18-month biotreatment is not possible. In soil S3; the 2-4/5-6 ratio is much higher than in soil S2 and decreases from 9.8 to 4.4 from the coarsest to the finest fraction, with an average value of 8.4 (Table 3).

Given that all three soils are strongly polluted with coal tar (Lors et al. 2010, 2011), tar concentration can be approximated from the total organic content of the soil, other sources of organic carbon being negligible compared to coal tar. The PAH concentration of coal tar particles was thus estimated by the PAH concentration of the soil divided by its total organic content (noted

thereafter PAHs/TOC). This ratio is low for all fractions, with an average value of 0.83% indicating a low PAH concentration in the remaining coal tar particles. Indeed, as the amounts of clay and organic matter are very low in soil S2, most of the PAHs remaining after biotreatment are entrapped in coal tar particles. The value of PAHs/TOC is higher in soil S3 than in soil S2, with an average value of 3.2% (Tables 2 and 3). Thus, despite similar total PAH concentrations in these soils, PAHs are more concentrated in the coal tar of soil S3. Additionally, soil S3 is also richer in 3- and 4-ring PAHs and poorer in 2-, 5- and 6- ring PAHs.

As expected, soil S3T that was subjected to a windrow-treatment has a lower PAH concentration than soil S3 whatever the fraction considered (Table 4). The windrow treatment did not modify the distribution of PAHs between the different soil fractions, most PAHs being still contained in the 200-2000 µm fraction (82%). The 2-4/5-6 ratios range from 1.4 to 4.0 according to fraction, with an average value of 2.6 compared to 8.4 for the untreated soil. The reported values indicate that 2- to 4-ring PAHs were more degraded than 5- to 6-ring PAHs during the biotreatment. This can be explained by the higher bioavailability of 2- to 4-ring PAHs in connection to their higher solubility (Bamforth and Singleton 2005). Nevertheless, despite of 6-month windrow treatment, soil S3T has a higher 2-4/5-6 ratio than soil S2 even after 18-month biotreatment, suggesting (in the absence of knowledge of initial values) that soil S2 is probably at a more advanced stage of bioremediation than soil S3T. However, despite that bioremediation is more advanced in soil S2, soil S3T has a value for PAHs/TOC lower than soil S2 (0.62% compared to 0.83%) and its total amount of PAHs is also lower than soil S2 that contains a greater amount of coal tar estimated by TOC. This suggests that soil S2 had been more heavily polluted than soil S3 before biotreatment. Additionally, the efficiency of the biotreatment applied to soil S3 can be assessed by a strong drop in PAHs/TOC value, from 3.2% to 0.6%. Some of the organic compounds contained in coal tar were thus degraded more slowly than PAHs or even not degraded at all.

Microscopic observations

The observation of the soil fractions above 200 µm was performed on polished sections instead of soil particles directly deposited on a sample holder. This method allows observing the internal microstructure of the particles as cross sections are made during polishing. Moreover, chemical analyses performed by EDS under SEM are more accurate on the flat surfaces of polished sections.

Microscopic observations by SEM of coarse grains of soil S2 indicate that most of them are aggregates of small particles showing a large array of sizes, generally from 1 to 500 µm, with

different levels of grey (Fig. 2a). These levels of grey are linked to the mean atomic weight of the compounds contained in the particles, darker levels corresponding to lower mean atomic weights. Thus, organic compounds (with a skeleton made of carbon, Ar = 12.01) are dark grey while mineral compounds (with a skeleton made of silicon in the present case, Ar = 28.09) are light grey. The resin, used to impregnate the soil before sectioning it, appears dark grey like organic compounds contained in soil particles.

Some organic compounds of soil S2 have angular shapes and are very homogeneous, without visible internal porosity. These angular shapes can be linked to the break-up of larger fragile particles, suggesting that these organic compounds are solid. Other organic particles have a smooth rounded shape and are seemingly composed of high-viscosity organic compounds liquid. Polished sections reveal the presence of a pore network that was not intruded by resin during preparation. Pores have a flat shape and a size most often smaller than 10 µm in diameter (Fig. 2b, enlargement of Fig. 2a). These two major types of organic particles cannot be differentiated by their chemical composition (EDS analysis): most carbon is found along with some oxygen and traces of sulphur, as frequently observed in coal tar or coke particles (Picon-Hernandez et al. 2008).

Soil S3 also presents some large grains made of smaller organic and mineral particles (Fig. 2c). Contrary to soil S2, most coal tar particles are lens shaped, in agreement with viscous organic compounds contained in quartziferous sandy soils (Vulava et al. 2007). Smaller soil grains are often mostly comprised of a unique coal tar particle finely covered with very small mineral particles glued to its surface (Fig. 2d). Almost all coal tar particles display a large porosity. Pore networks are most often filled by the resin intruded during the preparation. EDS chemical analysis was used to differentiate coal tar from resin, both showing almost identical grey levels: the resin contains chloride whereas coal tar contains sulphur. The presence of resin in the pores indicates that most pores are connected with the surface of coal tar particles. Some pores opening to the surface have been reported previously from the observation of the surface of coal tar or coke particles, the amount of pores varying markedly depending on origin and processing of the constituents (Panaitescu and Predeanu 2007; Picon-Hernandez et al. 2008).

At least two distinct organic compounds are associated with distinct porosities: one organic compound contains large pores (soil S3) and the other one is denser and displays a porosity looking like that of soil S2 (Fig. 2d). Some particles, called cenospheres, that can be almost entirely porous, were also observed by other authors (Panaitescu and Predeanu 2007; Ghosh et al. 2000).

In summary, the microstructure of coal tar is very heterogeneous with some anisotropy in agreement with previous observations by Panaitescu and Predeanu (2007). However, the present work demonstrates for the first time that the pores open to the surface are connected and thus that

pore water can be in contact with the internal porosity of coal tar particles. Observations in optical microscopy demonstrate even more easily the presence of a connected pore network (Fig. 2e). Here, the differentiation between coal tar and resin is obvious: organic compounds of coal tar appear in white with some mosaic patterns in relation to coal tar anisotropy while resin appears homogeneous with a medium grey level. The connected internal pore network of coal tar particles is thus well defined by grey-level differences between resin and coal tar organic compounds. Unconnected pores in which resin cannot penetrate are also well defined, appearing black. Optical microscopy, simpler and less expensive than SEM, can give satisfactory results when estimating the amount of porosity within coal tar particles. However, mineral compounds are not so well discriminated compared to SEM observations with a better contrast due to differences in mean atomic number. In addition, magnification is rapidly limited for optical microscopy compared to SEM.

SEM observations on soil S3T reveal, in agreement with the distribution of soil fractions (Table 1), that the biotreatment did not modify the initial size of coal tar particles. Like soil S3, soil S3T shows large coal tar particles engulfed in a matrix of small mineral grains (Fig. 2f). However, the volume of the internal pore network of coal tar particles was markedly increased by the biotreatment (Fig. 2g). In order to further assess the connection of the internal pore system of coal tar particles with soil water, polished sections of soil S3T were prepared with less pressure applied to the resin when embedding the soil, the internal pore system of coal tar particles being not always intruded by the resin. With this specific setup, it was possible to observe mineral particles in contact with pores open at the coal tar surface. This is an additional evidence of the presence of an open connected pore network that had developed over the whole volume of coal tar particles during biotreatment.

Image analysis indicated that coal tar particles of soil S2 have a small pore volume fraction of $6 \pm 1\%$ while pore volume fractions of $47 \pm 3\%$ and $65 \pm 4\%$ are found for soils S3 and S3T, respectively.

Discussion

Microscopic observations of coal tar particles brought some helpful additional data to previous ecotoxicological assays and chemical analyses (Lors et al. 2010, 2011), more especially by revealing the presence of a connected network of pores open to the surface that depended on the type of organic compounds contained in coal tar particles. When an open porosity was found, the coal tar surface potentially in contact with soil water was expected to increase markedly.

Additionally, the presence of an open porosity can be beneficial to speed up the rate of biodegradation of coal tar particles. Indeed, the biodegradation of coal tar particles increased the amount of porosity indicating that biodegradation occurred on the whole available surface of coal tar and thus even in the internal porosity of coal tar particles. The relative increase of porosity between soils S3 and S3T due to biotreatment was 1.38. This increase can be related to the microbial consumption of organic compounds (33 000 mg kg^{-1}) contained in coal tar particles. As the volume of coal tar particles remained constant, the proportion of consumption of coal tar can be related to the relative increase of porosity if the density of coal tar is known. Considering an average density of 1.3 for coal tar (Brown et al. 2006), the observed decrease of 36.6% of TOC would lead to increase the porosity of soil S3 by 1.28. This value compares well with 1.38 that corresponds to the relative increase of porosity between soils S3 and S3T.

The diffusion of pollutants and mostly PAHs from coal tar particles to soil water depends first on the gradient of PAH concentration between coal tar particles and soil water. Thus, ecoscores have been represented as a function of PAHs/TOC that gives an estimate of PAH concentration in coal tar particles rather than their concentration in bulk soil as presented in Fig 1. This estimate is expected to be pertinent for the three studied soils due to their low content in clay and organic matter, known for having high sorptive affinities to PAHs (Lamichlane et al. 2016). Ecoscores increase with PAHs/TOC: soil S2 now ranges between soils S3 and S3T (Fig. 3, compare with Fig. 1). Thus, PAH concentration in coal tar particles differentiates soil S2 from soil S3 despite a similar concentration of PAHs in both soils. Despite a strong hazard potential, soil S2 gave a moderate ecotoxic response as its coal tar particles exhibited a small internal pore volume. This comparison of ecoscores and microscopic observations also confirms that analytical results of solvent extracts are not representative of environmental hazard of PAH-polluted soils (Semple et al. 2003).

The amount of internal porosity of coal tar particles can also indicate the best strategy for remediation. Indeed, if this amount is low, other techniques than biodegradation may be preferred. The advancement of a biotreatment can also be surveyed by the increase of the internal porosity of coal tar particles in relation to the biodegradation of organic compounds. Moreover, the value of internal porosity can be used as a criterion to determine when the biotreatment can be ended. Despite the necessary statistical approach of microscopy, this technique is the only one that can assess quantitatively and qualitatively the porosity of coal tar particles. Other techniques, such as mercury intrusion porosimetry or adsorption isotherm measurements, are not able to differentiate the surface of organic compounds relative to that of mineral compounds contained in the soil.

Conclusion

As already known, the assessment of the environmental hazard of soils polluted by NAPLs and especially by coal tar is complex and a multi-disciplinary approach is thus required. The bioavailability of PAHs is linked to their rates of desorption from coal tar particles to the soil water that depends first on diffusion but also on additional mechanisms. The diffusion of PAHs to soil water can be correlated to the PAH concentration in coal tar particles. It can be estimated in the case of the reported sandy soils by the overall ratio between PAH concentration and the total organic content. Indeed, ecoscores increase almost linearly with PAH concentration in coal tar particles, although this relationship should be verified on a wider array of soils. The rate of release of PAHs is linked to additional parameters, such as the surface area of coal tar in contact with soil water. Microscopic observations of the coarser fraction (> 200 µm) of two of the three studied soil samples showed an interconnected pore network opening to the surface of coal tar particles. Biotreatment increased the amount of porosity due to the microbial consumption of some organic compounds contained in coal tar particles. The presence of a pore network increases markedly the surface area of coal tar in contact with soil water and thus the potential release rate of pollutants. Thus, microscopy can be an additional method to chemical analyses and ecotoxicological assays to assess the best strategy for remediation but also to follow the efficiency of a biotreatment. Our study also confirmed that the analysis of PAHs transferred to the water fraction using water instead of solvent extraction could be advised in the perspective of environmental hazard assessment.

Acknowledgements The present study was performed with a financial support from the ADEME (Agence de l'Environnement et de la Maîtrise de l'Énergie, France), which is greatly acknowledged. We thank Total (France) and Charbonnages de France (France) to put industrial sites at our disposal.

References

Al-Raoush RI (2014) Experimental investigation of the influence of grain geometry on residual NAPL using synchrotron microtomography. J Contamin Hydrol 159:1–10. doi: 10.1016/j.jconhyd.2014.01.008

Bamforth SM, Singleton I (2005) Bioremediation of polycyclic aromatic hydrocarbons: current knowledge and future directions. J Chem Technol Biotechnol 80:723–736. doi: 10.1002/jctb.1276

Benhabib K, Faure P, Sardin M, Simonnot MO (2010) Characteristics of a solid coal tar sampled from a contaminated soil and the organics transferred into water. Fuel 89:325–359. doi: 10.1016/j.fuel.2009.06.009

Brown DG, Gupta L, Kim TH, Moo-Young HK, Coleman AJ (2006) Comparative assessment of coal tars obtained from 10 former manufactured gas plant sites in the Eastern United States. Chemosphere 62:562–1569. doi: 10.1016/j.chemosphere.2006.03.068

Chung N, Alexander M (2002) Effect of soil properties on bioavailability and extractability of phenanthrene and atrazine sequestered in soil. Chemosphere 48:109–115. doi: 10.1016/S0045-6535(02)00045-0

Eom IC, Rast C, Veber AM, Vasseur P (2007) Ecotoxicity of a polycyclic aromatic hydrocarbon (PAH)-contaminated soil. Ecotoxicol Environ Saf 67:190–205. doi: 10.1016/j.ecoenv.2006.12.020

EPRI (1993) Chemical and physical characteristics of tar samples from selected manufactured gas plant (MGP) sites. http://www.hawaiidoh.org/references/EPRI%201993.pdf. Accessed 13 April 2017

Ghosh U, Gillette JS, Luthy RG, Zare RN (2000) Microscale location, characterization, and association of polycyclic aromatic hydrocarbons on harbor sediment particles. Environ Sci Technol 34:1729–1736. doi: 10.1021/es991032t

Hu C, Ma H (2016) Statistical analysis of backscattered electron image of hydrated cement paste. Advances in Cement Research 28(7):469–474. doi: 10.1680/jadcr.16.00002

ISO (1995) ISO 10694. Soil quality. Determination of organic carbon and total carbon after dry combustion (elementary analysis). International Organization for Standardization, Geneva.

ISO (1998) ISO 13877. Soil quality. Determination of polynuclear aromatic hydrocarbons. method using high-performance liquid chromatography. International Organization for Standardization, Geneva.

Johnsen AR, Wick YL, Harms H (2005) Principles of microbial PAH-degradation in soil. Environ Pollut 133:71–84. doi: 10.1016/j.envpol.2004.04.015

Igarashi S, Kawamura M, Watanabe A (2004) Analysis of cement pastes and mortars by a combination of backscatter-based SEM image analysis and calculations based on the Powers model. Cem Concr Compos 26: 977–985. doi: 10.1016/j.cemconcomp.2004.02.031

354 Lamichlane S, Krishna KCB, Sarukkalige R (2016) Polycyclic aromatic hydrocarbons (PAHs)
355 removal by sorption: a review. Chemosphere 148:336–353.
356 doi: /10.1016/j.chemosphere.2016.01.036

357 Lors C, Ponge JF, Damidot D (2010) Comparison of solid-phase bioassays and ecoscores to
358 evaluate the toxicity of contaminated soils. Environ Pollut 158:2640–2647.
359 doi: 10.1016/j.envpol.2010.05.005

360 Lors C, Ponge JF, Damidot D (2011) Comparison of solid and liquid-phase bioassays using
361 ecoscores to assess contaminated soils. Environ Pollut 159:2974–2981.
362 doi: 10.1016/j.envpol.2011.04.028

363 Lors C, Ponge JF, Damidot D (2017) Environmental hazard assessment by the Ecoscore system to
364 discriminate PAH-polluted soils. Environ. Sci. Pollut. Res. (in press). doi: 10.1007/s11356-
365 017-9906-4

366 Mahjoub B, Jayr E, Bayard R, Gourdon R (2000) Phase partition of organic pollutants between
367 coal tar and water under variable experimental conditions. Water Res 34:3551–3560.
368 doi: 10.1016/S0043-1354(00)00100-7

369 Nambi MN, Powers SE (2000) NAPL dissolution in heterogeneous systems: an experimental
370 investigation in a simple heterogeneous system. J Contamin Hydrol 44:161–184.
371 doi: 10.1016/S0169-7722(00)00095-4

372 Panaitescu C, Predeanu G (2007) Microstructural characteristics of toluene and quinoline-
373 insolubles from coal-tar pitch and their cokes. Int J Coal Geol 71:448–454.
374 doi: 10.1016/j.coal.2006.11.003

375 Peijnenburg W, Sneller E, Sijm D, Ljizen J, Traas T, Verbruggen E (2002) Implementation of
376 bioavailability in standard setting and risk assessment. J Soils Sediments 2:169–173.
377 doi: 10.1007/BF02991036

378 Picon-Hernandez HJ, Centeno-Hurtado A, Pantoja-Agreda E.F (2008) Morphological classification
379 of coke formed from the Castilla and Jazmín crude oils. Cienc Tecnol Futuro 3:169–183.

380 Rhodes AH, Carlin A, Semple KT (2008) Impact of black carbon in the extraction and
381 mineralization of phenanthrene in soil. Environ Sci Technol 42:740–455.
382 doi: 10.1021/es071451n

383 Riding MJ, Doick KJ, Martin FL, Jones KC, Semple K.T (2013) Chemical measures of
384 bioavailability/bioaccessibility of PAHs in soil: fundamentals to application. J Hazard

Mater 261:687–700. doi: 10.1016/j.jhazmat.2013.03.033

Semple KT, Morriss AWJ, Paton GI (2003) Bioavailability of hydrophobic organic contaminants in soils: fundamental concepts and techniques for analysis. Eur J Soil Sci 54:809–818. doi: 10.1046/j.1351-0754.2003.0564.x

Thiele-Bruhn S, Brümmer GW (2004) Fractionated extraction of polycyclic aromatic hydrocarbons (PAHs) from polluted soils: estimation of the PAH fraction degradable through bioremediation. Eur J Soil Sci 55:567–578. doi: 10.1111/j.1365-2389.2004.00621.x

Vulava VM, McKay LD, Driese SG, Menn FM, Sayler GS (2007) Distribution and transport of coal tar-derived PAHs in fine-grained residuum. Chemosphere 68:554–563. doi: 10.1016/j.chemosphere.2006.12.086

Vulava VM, McKay LD, Broholm MM, McCarthy JF, Driese SG, Sayler GS (2012) Dissolution and transport of coal tar compounds in fractured clay-rich residuum. J Hazard Mater 203/204:283–289. doi: 10.1016/j.jhazmat.2011.12.023

White PA, Claxton LD (2004) Mutagens in contaminated soil: a review. Mutat Res 567:227–345. doi: 10.1016/j.mrrev.2004.09.003

401 **Figure captions**

402 **Fig. 1.** Ecoscores as a function of total PAH concentration of soil. Ecoscores were calculated from
403 a reduced battery of bioassays (Lors et al. 2011) that was normalized to 100%.

404 **Fig. 2.** Micrographs of studied soils in scanning electron microscopy. a) Soil S2 in scanning
405 electron microscopy; b) Soil S2 in scanning electron microscopy, enlargement of the central
406 organic particle of Figure 2a; c) Soil S3 in scanning electron microscopy; d) Soil S3 in scanning
407 electron microscopy, other view; e) Soil S3 in optical microscopy; f) Soil S3T in scanning electron
408 microscopy; g) Soil S3T in scanning electron microscopy, other view.

409 **Fig. 3.** Relation between ecoscores and ratios of PAH concentration over total organic
410 concentration (PAHs/TOC) in the three studied soils. Ecoscores were calculated from a reduced
411 battery of bioassays (Lors et al. 2011) that was normalized to 100% similarly to Figure 1.

412

Figure captions

Fig. 1. Ecoscores as a function of total PAH concentration of soil. Ecoscores were calculated from a reduced battery of bioassays (Lors et al. 2011) that was normalized to 100%.

Fig. 2. Micrographs of studied soils in scanning electron microscopy. a) Soil S2 in scanning electron microscopy; b) Soil S2 in scanning electron microscopy, enlargement of the central organic particle of Figure 2a; c) Soil S3 in scanning electron microscopy; d) Soil S3 in scanning electron microscopy, other view; e) Soil S3 in optical microscopy; f) Soil S3T in scanning electron microscopy; g) Soil S3T in scanning electron microscopy, other view.

Fig. 3. Relation between ecoscores and ratios of PAH concentration over total organic concentration (PAHs/TOC) in the three studied soils. Ecoscores were calculated from a reduced battery of bioassays (Lors et al. 2011) that was normalized to 100% similarly to Figure 1.

Figure

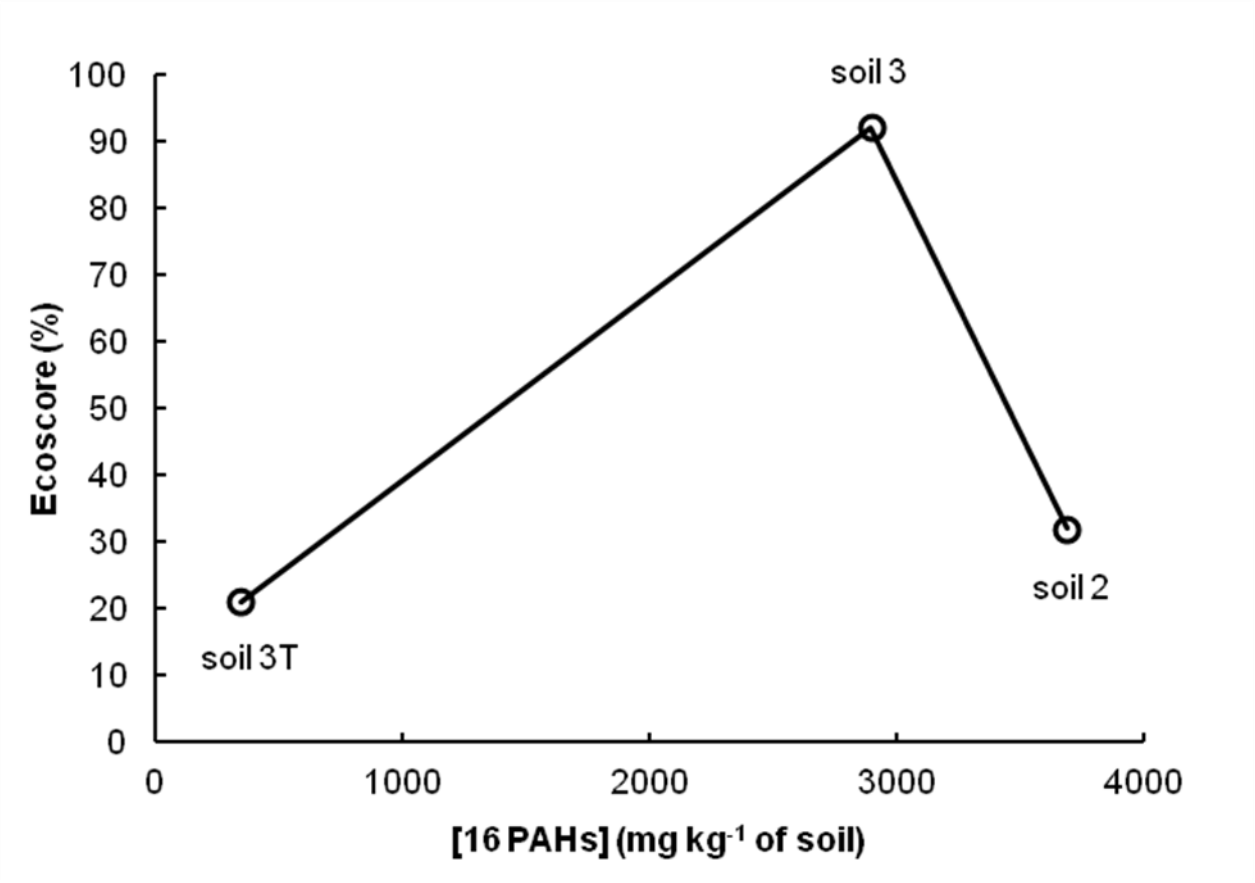
100
90
80
70
60
50
40
30
20
10
0
Ecoscore (%)
soil 3
soil 2
soil 3T
0
1000
2000
3000
4000
[16 PAHs] (mg kg-1 of soil)

Fig. 1

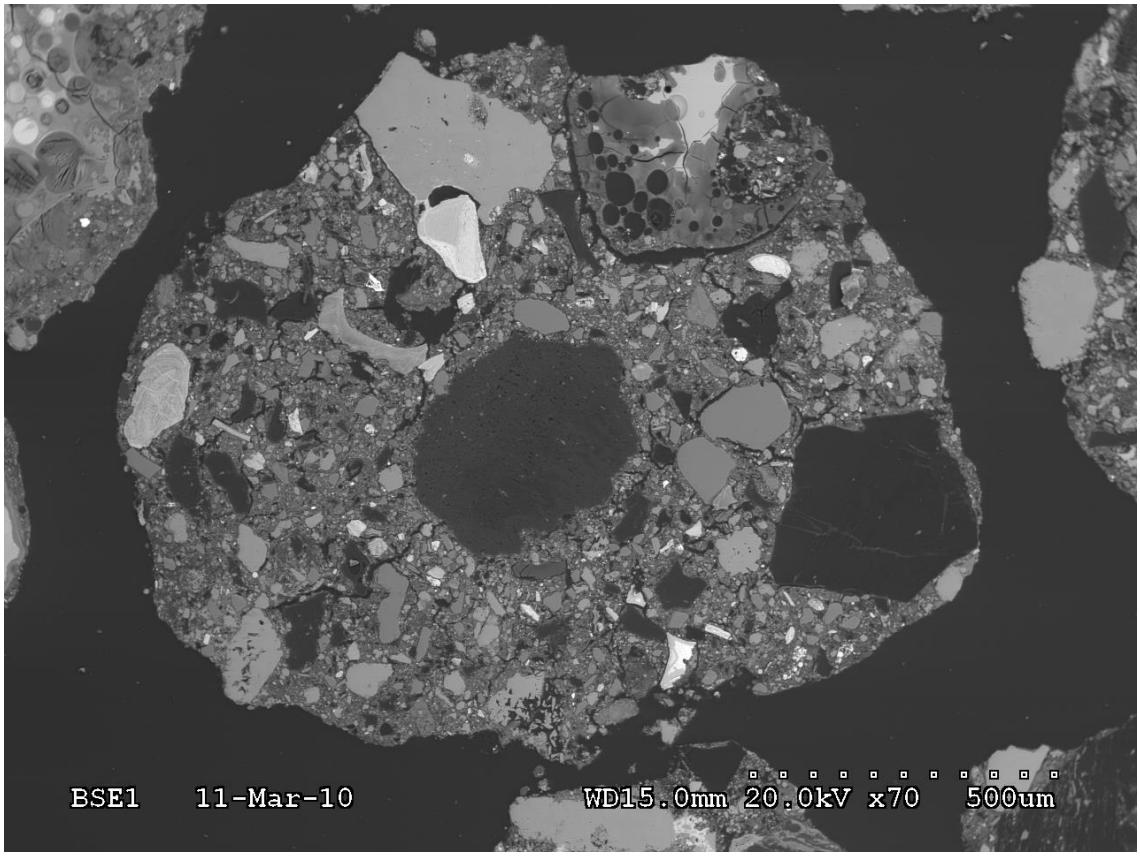

Fig. 2a

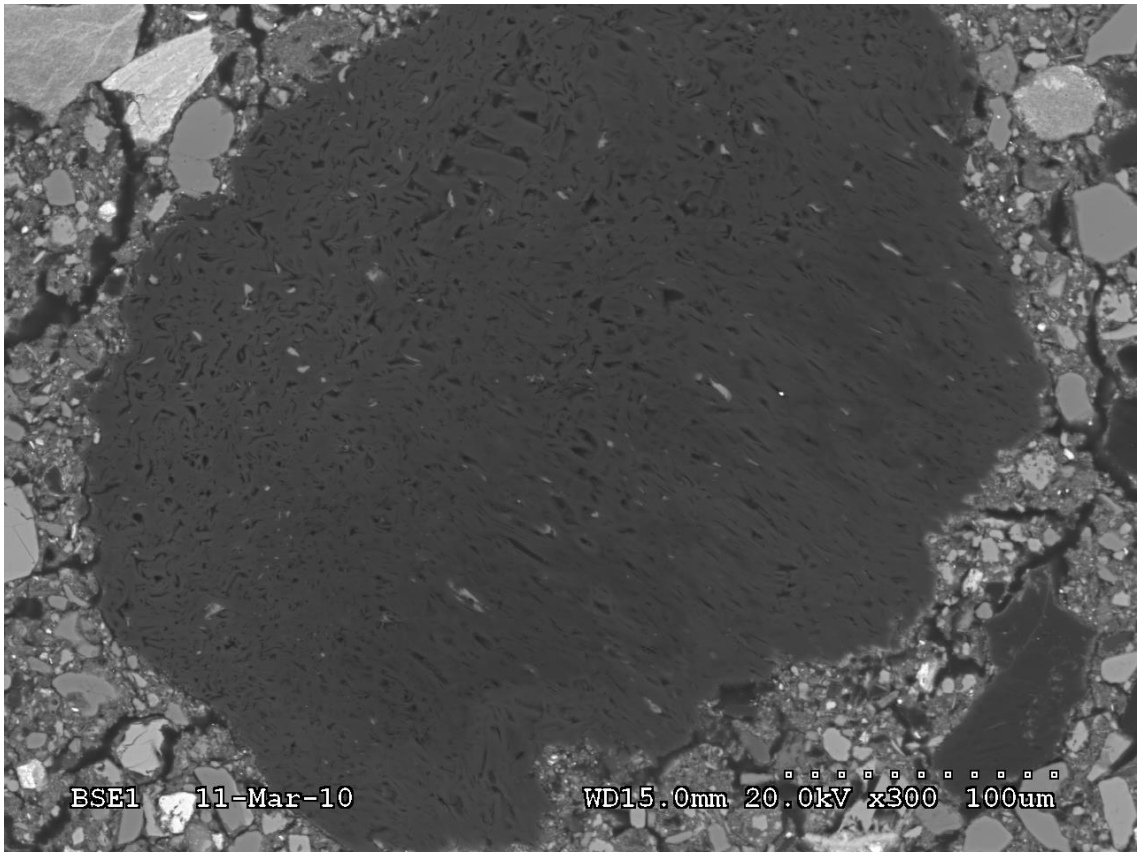

Fig. 2b

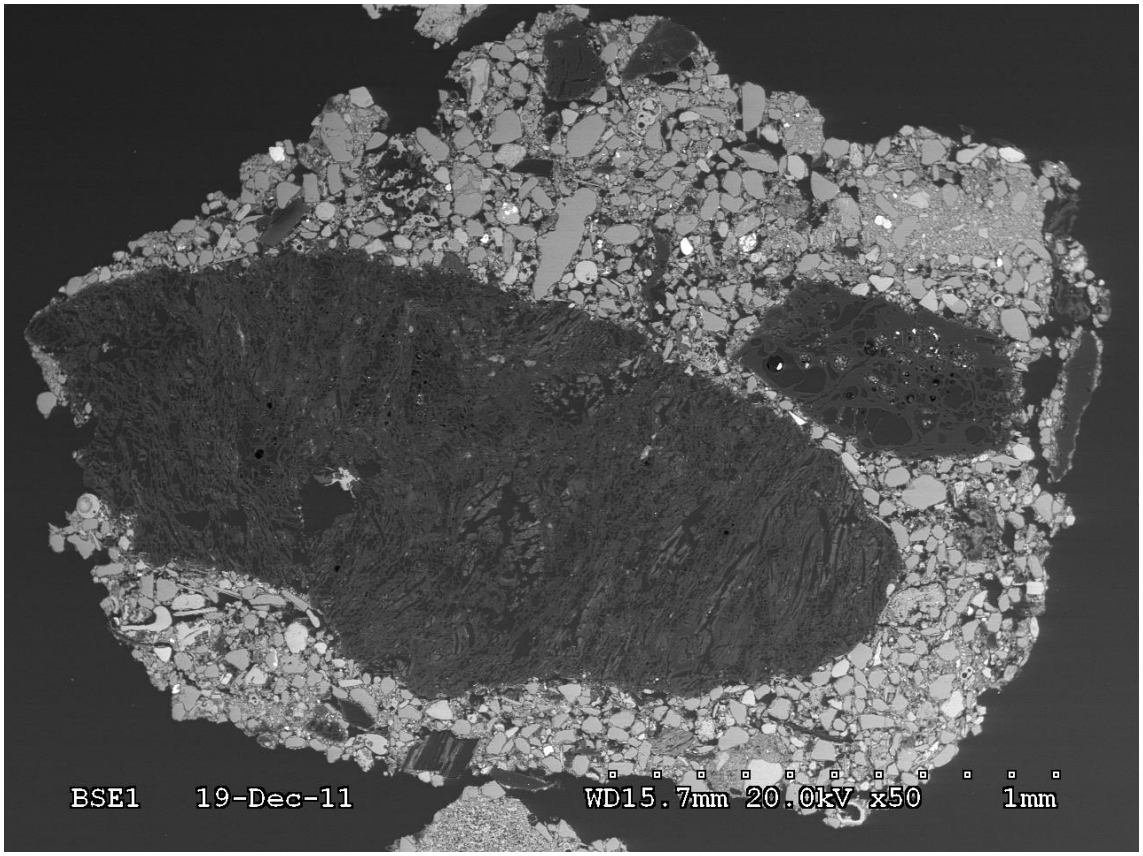

Fig. 2c

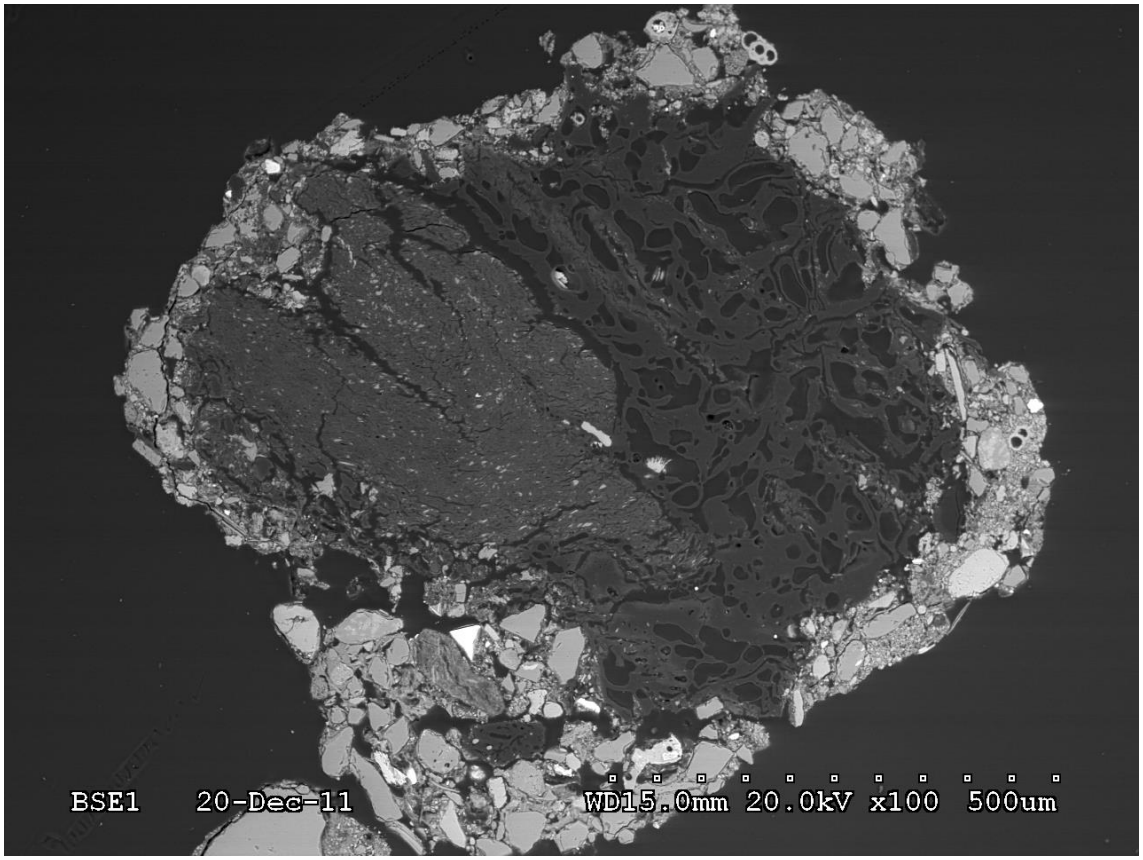

Fig. 2d

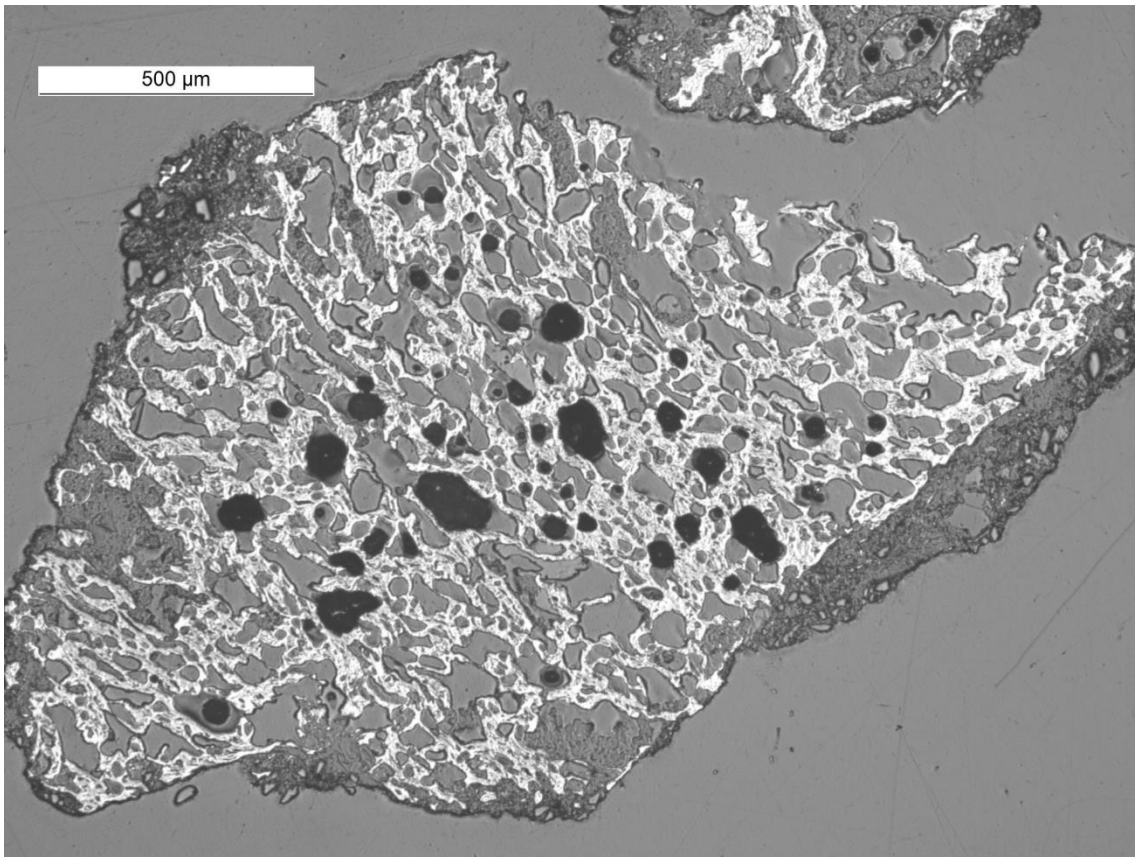

Fig. 2e

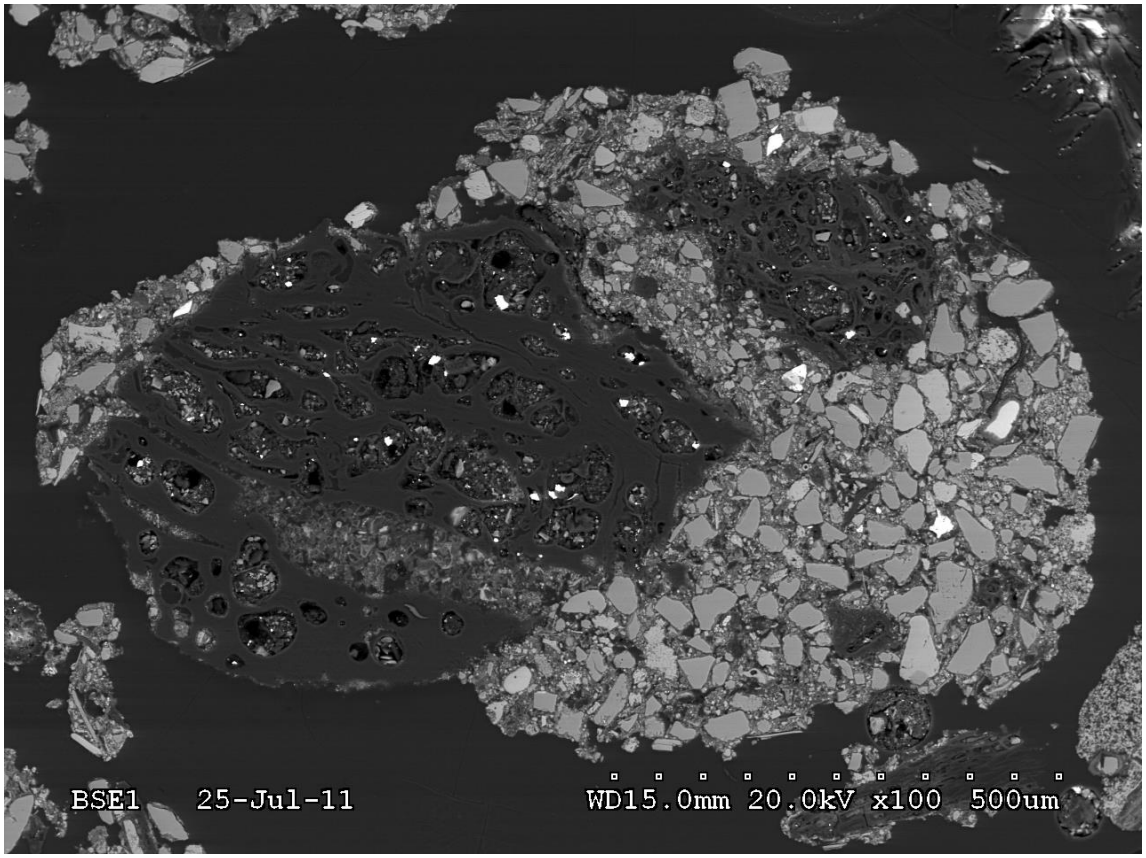

Fig. 2f

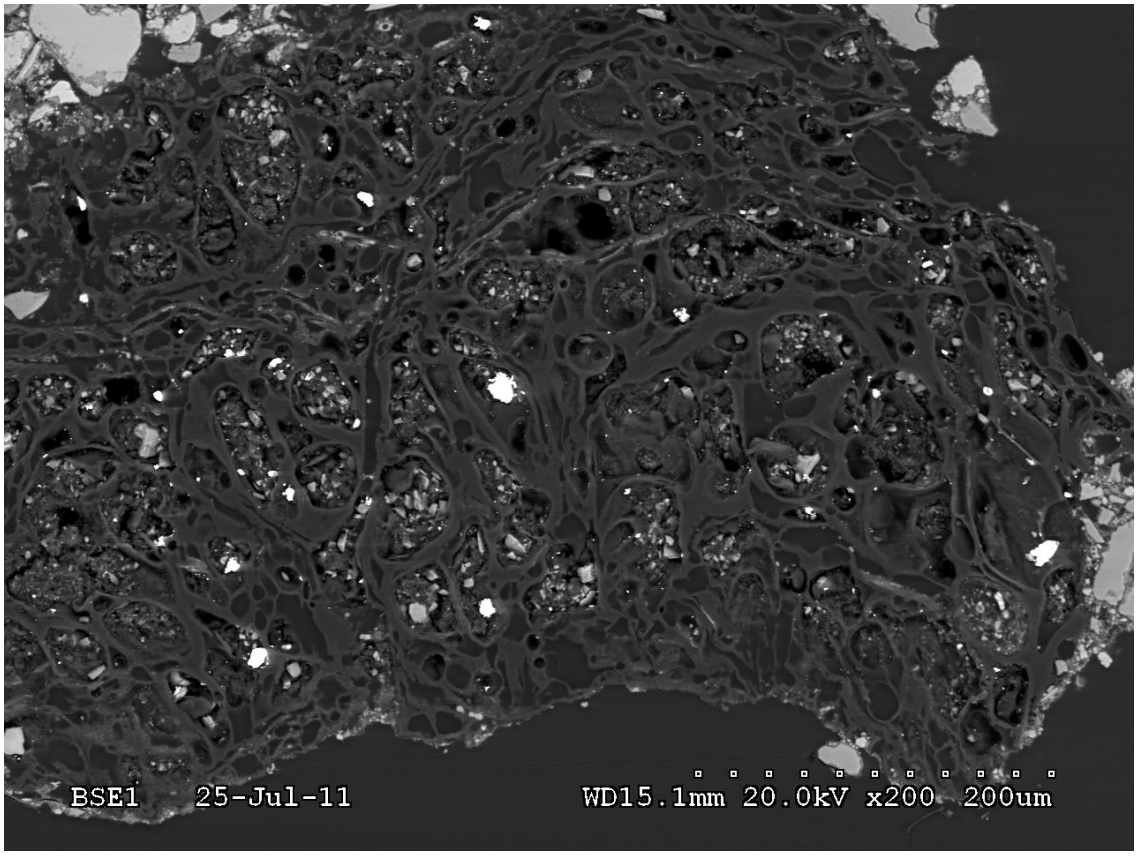

Fig. 2g

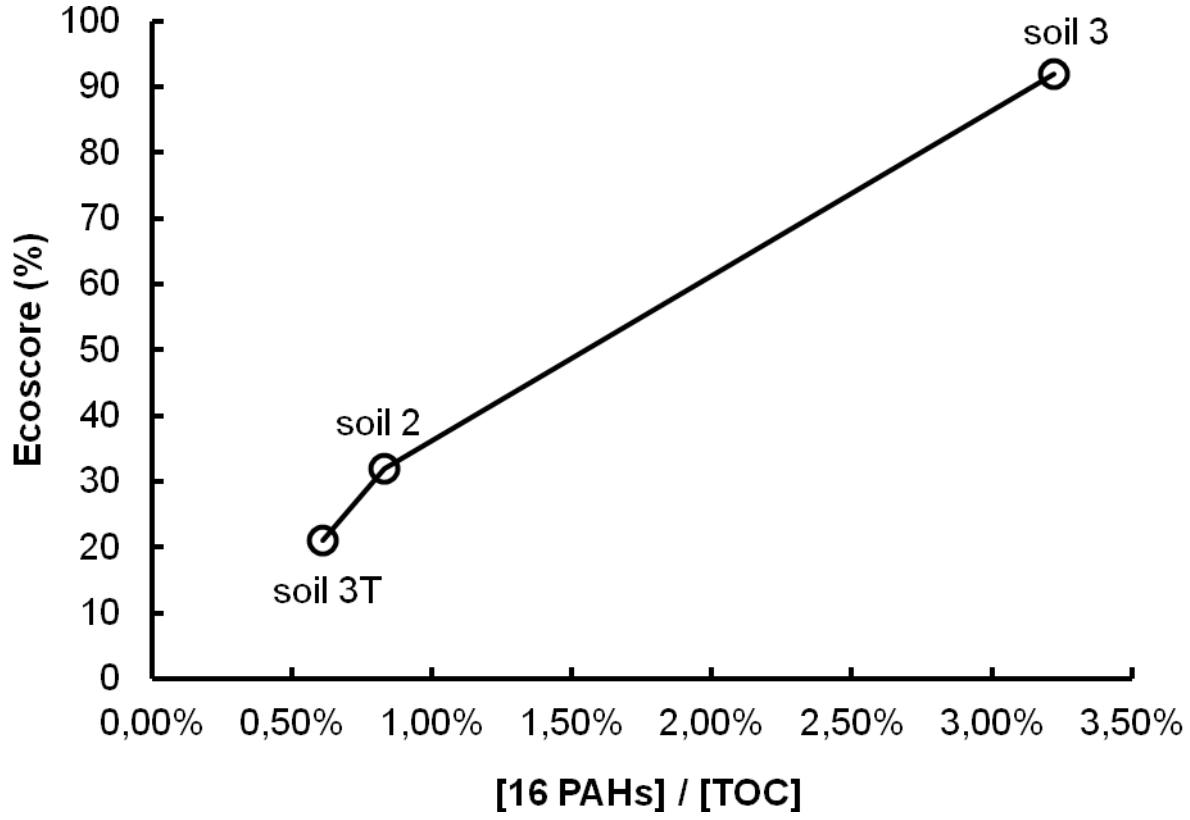
100
90
80
70
60
50
40
30
20
10
0
Ecoscore (%)
soil 3
soil 2
soil 3T
0,00%
0,50%
1,00%
1,50%
2,00%
2,50%
3,00%
3,50%
[16 PAHs] / [TOC]

Fig. 3

Table

Table 1. Distribution of soil particle size fractions (in mass %) in the three studied soils.

Soil fractions	S2	S3	S3T
> 2000 mm	17.19	9.14	9.12
2000-200 µm	55.84	67.93	67.82
200 - 50 µm	23.41	18.16	18.14
50 - 20 µm	1.59	3.05	3.16
20 - 2 µm	1.72	1.39	1.44
< 2 µm	0.25	0.32	0.33

Table 2. PAH and total organic carbon concentrations in each fraction of soil S2.

	soil fraction (µm)						
Concentration (mg kg^{-1} of soil)	**> 2000**	**2000-200**	**200-50**	**50-20**	**20-2.**	**< 2**	**Soil = Σ fractions**
2 ring PAHs	41.6	247.5	109.2	6.2	14.0	1.9	420
3 ring PAHs	191.2	669.0	229.2	8.0	20.4	1.1	1 119
4 ring PAHs	28.3	223.3	97.1	4.2	10.7	0.1	364
5 ring PAHs	100.5	584.7	299.1	9.9	29.3	2.8	1 026
6 ring PAHs	68.4	430.2	228.2	7.3	22.3	1.6	758
Total PAHs	430	2 155	963	36	97	7	3 687
distribution of PAHs	11.66%	58.44%	26.11%	0.96%	2.62%	0.20%	100%
TOC	42 013	325 066	66 786	3 230	4 211	693	442 000
2-4 / 5-6 ratio	1.55	1.12	0.83	1.06	0.88	0.7	1.07
PAHs / TOC (%)	1.02	0.66	1.44	1.10	2.30	1.07	0.83

Table 3. PAH and total organic carbon concentrations in each fraction of soil S3.

	soil fraction (µm)						
concentration (mg kg^{-1} of soil)	**> 2000**	**2000-200**	**200-50**	**50-20**	**20-2**	**< 2**	**Soil = Σ fractions**
2 rings PAHs	2.5	65.3	8.1	0.4	0.4	0.0	77
3 rings PAHs	47.1	1 120.0	141.5	1.3	7.2	3.6	1 321
4 rings PAHs	41.0	1 000.4	129.7	3.3	8.7	7.6	1 191
5 rings PAHs	6.8	179.2	23.3	0.4	1.9	1.6	213
6 rings PAHs	2.5	79.0	9.7	0.2	1.2	1.0	94
Total PAHs	100	2 444	312	6	19	14	2 895
Distribution of PAHs	3.45%	84.42%	10.78%	0.19%	0.67%	0.48%	100%
TOC	6 325	77 617	5 146	335	396	181	90 000
2-4 / 5-6 ratio	9.78	8.47	8.48	8.55	5.31	4.37	8.44
PAHs / TOC (%)	1.58	3.15	6.07	1.68	4.90	7.65	3.22

Table 4. PAH and total organic carbon concentrations in each of soil S3T.

	soil fraction (µm)						
concentration (mg kg^{-1} of soil)	**> 2000**	**2000-200**	**200-50**	**50-20**	**20-2**	**< 2**	**Soil = Σ fractions**
2 ring PAHs	1.1	19.3	2.5	0.2	0.2	0.0	23
3 ring PAHs	4.1	48.7	4.5	0.2	0.3	0.2	58
4 ring PAHs	8.0	141.2	15.9	0.4	1.2	0.8	168
5 ring PAHs	2.6	51.2	6.6	0.1	0.5	0.4	62
6 ring PAHs	1.2	22.8	10.4	0.1	0.2	0.2	35
Total PAHs	17	283	40	1	2	2	345
distribution of PAHs	4.94%	82.03%	11.55%	0.30%	0.70%	0.48%	100%
TOC	4 448	43 263	7 617	900	490	282	57 000
2-4 / 5-6 ratio	3.47	2.83	1.35	3.96	2.17	1.68	2.58
PAHs / TOC (%)	0.39	0.67	0.54	0.12	0.50	0.60	0.62